

Detection of Cognitive Binding During Ambiguous Figure Tasks by Wavelet Coherence Analysis of EEG Signals

Ta-Hsin Li*

Dept. of Statistics & Applied Probability
University of California
Santa Barbara, CA 93106, USA

William R. Klemm

Dept. of Veterinary Anatomy & Public Health
Texas A&M University
College Station, TX 77843, USA

Abstract

It is hypothesized that the perception of an alternative image in ambiguous figures would be manifested as an increase in synchronization of EEG signals over multiple scalp sites as “cognitive binding” occurs. A statistical time-frequency analysis (STFA) approach is taken to detect cognitive binding. The STFA approach consists of an analysis filter bank that extracts useful components from the input EEG signals and certain statistical parameters at the output that characterize the synchronization patterns over multiple scalp sites. With the help of wavelet-packet filters and wavelet coherence measures, cognitive binding is detected over many frequency bands by statistical testing.

1. Introduction

Synchronized (or coherent) oscillatory patterns in multiple electroencephalographic (EEG) signals have been found in many studies as manifestation of different mental activities [1]–[4]. This research focuses on detecting possible neural mechanisms of “cognitive binding”—a process by which humans recognize spatially distributed elements of a stimulus, detect salient relationships, and bind them into a meaningful and coherent whole.

Ambiguous figures are considered as a convenient way to induce cognitive binding. Ambiguous figures have two different and mutually exclusive perceptions. The familiar “Batman” logo, for example, is an ambiguous figure because it can be perceived either as the black representation of a bat or as a set of white teeth. By Gestalt theory [5], a subject looking at an ambiguous figure will preferentially perceive a “default” image without particular mental effort, and only with sustained thinking via cognitive binding does the subject realize the existence of an alternative image. It is

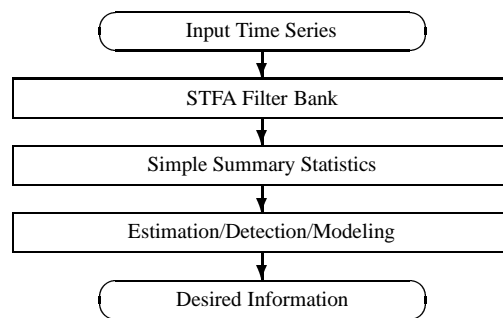


Figure 1. Schema of the STFA approach.

hypothesized in this research that the perception of an alternative image in ambiguous figures would be manifested as an increase in synchronization of EEG signals over multiple scalp sites as cognitive binding occurs.

2. The STFA Approach

To test the hypothesis, we employ a general time series analysis approach called statistical time-frequency analysis (STFA) [6]. As depicted in Fig. 1, STFA combines an analysis filter bank with simple summary statistics at the output for time series analysis [6]. The role of the filter bank (or parametric filter) is to extract useful components from the input time series and suppress unwanted interference and noise; the role of the summary statistics at the output is to extract relevant statistical information from the output time series for detection, estimation, and modeling.

In this research, the filter bank comprises the finite impulse response (FIR) filters that produce the undecimated wavelet-packets (WP) transform [7], and the summary statistics at the output are taken to be the ordinary and partial correlation coefficients over multiple scalp sites, which we refer to as *wavelet coherence* and *wavelet partial coherence*. Unlike the traditional spectral coherence [4], [8], the wavelet coherence describes the correlation of

*Now with Department of Mathematical Sciences, IBM T. J. Watson Research Center, Yorktown Heights, NY 10598 (thl@watson.ibm.com).

multiscale wavelet components rather than fixed-scale sinusoidal components of the EEG signals. Wavelet-based methods have been proved effective in EEG signal processing for transient detection and classification [9], [10]. It is proved useful in this research for coherence analysis.

3. The EEG Data

The EEG data in this research were collected from 17 subjects. Each subject was presented with 10 ambiguous figure trials. Two segments of EEG signals, each being 1.28 sec. long (256 samples at 200 Hz rate), were recorded simultaneously at 19 scalp sites. The first segment was obtained at the beginning when the subject was just presented with an ambiguous figure. It represents the brain activity when the default image is perceived by the subject. The second segment was recorded when the subject managed to see the alternative image. It should capture the brain activity as cognitive binding occurs. All the EEG data were ensured to be free of artifacts by visual inspection. More information about the data can be found in [11].

4. Wavelet Coherence

Let $\{X_{it}\}_{t=1}^n$ denote a segment of (zero-mean) EEG signal obtained by the i th electrode ($i = 1, \dots, p$), and let $\mathcal{W}(\cdot)$ denote a WP filtering operator. Then, the output signal can be expressed as $Y_{it} := Y_{it}(\mathcal{W}) := \mathcal{W}(X_{it})$. We define the wavelet coherence between the i th and j th EEG signals for the given filter \mathcal{W} as

$$r_{ij} := r_{ij}(\mathcal{W}) := \text{Corr}(Y_{it}, Y_{jt}), \quad (1)$$

and define the wavelet partial coherence between the i th and j th EEG signals for the given filter \mathcal{W} as

$$\rho_{ij} := \rho_{ij}(\mathcal{W}) := \text{Corr}(Y_{it}, Y_{jt} \mid Y_{kt}, \forall k \neq i, j). \quad (2)$$

Assuming the EEG signals are multivariate normal random variables, ρ_{ij} can be computed recursively from r_{ij} [12]. One can regard ρ_{ij} as the ordinary correlation coefficient between the two residual time series obtained from the best linear estimates of Y_{it} and Y_{jt} , respectively, on the basis of the remaining variables $\{Y_{kt}, \forall k \neq i, j\}$.

Besides being a correlation coefficient, the wavelet coherence has at least three additional interpretations. First, r_{ij}^2 is equal to the proportion of the variability of Y_{it} that can be accounted for by its linear association with Y_{jt} . Second, under the multivariate normality assumption, $\xi_{ij} := \arccos(r_{ij})/\pi$ is equal to the expected zero-crossing rate of the interleaved time series $\{Z_t\}$ defined by $Z_{2t} := Y_{it}$ and $Z_{2t+1} := Y_{jt}$. Finally, under the normality assumption, $\eta_{ij} := 1 - \arccos(r_{ij})/\pi = 1 - \xi_{ij}$ is equal to the probability of $Y_{it}Y_{jt}$ exceeding zero, i.e., $P(Y_{it}Y_{jt} > 0)$.

All these quantities measure the degree of synchronization between two oscillatory signals from different aspects. The second and third interpretations, in particular, give rise to an alternative definition of wavelet coherence in terms of zero-crossing rate or zero-exceeding probability, i.e.,

$$r_{ij}^* := r_{ij}^*(\mathcal{W}) := \cos(\pi\xi_{ij}) = \cos(\pi - \pi\eta_{ij}). \quad (3)$$

This definition is different from (1) when the normality is invalid; it is equivalent to (1) when the normality holds.

Given $\{Y_{it}\}_{t=1}^n$ and $\{Y_{jt}\}_{t=1}^n$, one can estimate r_{ij} by the sample correlation coefficient $\hat{r}_{ij} := \sum(Y_{it} - \bar{Y}_i)(Y_{jt} - \bar{Y}_j) / \sqrt{\sum(Y_{it} - \bar{Y}_i)^2 \sum(Y_{jt} - \bar{Y}_j)^2}$, where \bar{Y}_i and \bar{Y}_j are the sample mean of Y_{it} and Y_{jt} , respectively. Substituting r_{ij} by \hat{r}_{ij} in the recursive algorithm in [12] produces $\hat{\rho}_{ij}$ as an estimate of ρ_{ij} . One can estimate r_{ij}^* by $\hat{r}_{ij}^* := \cos(\pi\hat{\xi}_{ij})$, where $\hat{\xi}_{ij} := n^{-1} \sum I\{(Y_{it} - \bar{Y}_i)(Y_{jt} - \bar{Y}_j) < 0\}$ with $I(\cdot)$ being the indicator function.

Wavelet coherence depends on the WP filters indexed by a binary code of length ℓ . If f_s is the sampling frequency, then, for a given code $m := (m_1, \dots, m_\ell)$, the WP filter \mathcal{W}_m has an effective passband in (f_{1m}, f_{2m}) , where $f_{1m} := \delta_\ell \sum_{i=1}^\ell m_i 2^{\ell-i}$, $f_{2m} := f_{1m} + \delta_\ell$, and $\delta_\ell := 2^{-\ell-1} f_s$.

5. Detection of Synchronized Patterns

Synchronized spatial patterns in the EEG signals can be detected by statistical hypothesis testing procedures based on the wavelet coherence measures of repeated trials. More precisely, suppose that the EEG signals are available for $K := K_s \times K_f$ independent trials from K_s subjects, each presented with K_f ambiguous figures. Let \hat{r}_{ijk} be the wavelet coherence from the k th trial. Under certain mixing conditions, one can show that $\hat{z}_{ijk} := \tanh^{-1}(\hat{r}_{ijk})$ is asymptotically normal with mean $z_{ij} := \tanh^{-1}(r_{ij})$ and variance $n^{-1}\sigma_{ij}^2$ for some σ_{ij}^2 [8]. Therefore, one can test for nonzero wavelet coherence by using the test statistic $t_{ij} := \sqrt{K} \bar{z}_{ij}/s_{ij}$, where \bar{z}_{ij} is the sample mean and s_{ij}^2 is the sample variance of $\{\hat{z}_{ijk}\}_{k=1}^K$. Under the null hypothesis of $r_{ij} = 0$, t_{ij} has an asymptotic T distribution with $K - 1$ degrees of freedom. Therefore, a T test would be able to detect significant coherence between the two sites.

Since $\hat{\zeta}_{ijk} := \tanh^{-1}(\hat{\rho}_{ijk})$ has an asymptotic normal distribution with mean $\zeta_{ijk} := \tanh^{-1}(\rho_{ijk})$, a similar T test can be used to test for the hypothesis of nonzero wavelet partial coherence (i.e., $\rho_{ij} = 0$ vs. $\rho_{ij} \neq 0$).

Fig. 2 shows some examples of wavelet coherence and partial coherence maps. Almost all pairs of EEG signals exhibit significant positive coherence in both segments and multiple frequency bands. The significant partial coherence reveals the synchronization patterns more clearly because the interference from the other sites is removed.

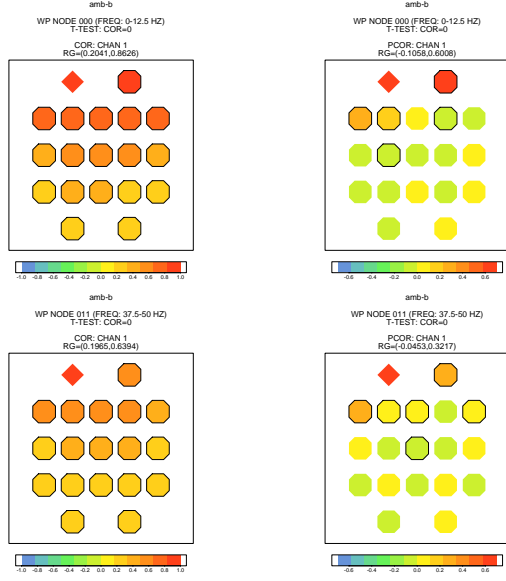


Figure 2. Wavelet coherence and partial coherence maps of the ambiguous figure experiment. Left: plot of $\hat{r}_{1j} := \tanh(\hat{z}_{1j})$. Right: plot of $\hat{\rho}_{1j} := \tanh(\hat{\zeta}_{1j})$. Top: obtained by \mathcal{W}_{000} (0–12.5 Hz). Bottom: obtained by \mathcal{W}_{011} (37.5–50 Hz). Symbols outlined in black indicate significant coherence at level 0.01.

6. Synchronization Change Detection

A paired T test can be applied to each pair of electrodes to test for the hypothesis of change in synchronization during cognitive binding. The paired T tests are performed on the difference between the transformed wavelet coherence of the two EEG segments. More precisely, let $\hat{z}_{ijk}^{(a)}$ and $\hat{z}_{ijk}^{(b)}$ denote the transformed wavelet coherence of segment 1 (*a priori*) and segment 2 (*binding*), respectively. Then, the test statistic can be expressed as $\tau_{ij} := \sqrt{K} \hat{z}_{ij}^{(d)} / s_{ij}^{(d)}$, where $\hat{z}_{ij}^{(d)}$ and $s_{ij}^{(d)}$ are the sample mean and the sample standard deviation of $\hat{z}_{ijk}^{(d)} := \hat{z}_{ijk}^{(b)} - \hat{z}_{ijk}^{(a)}$. The T test is justified by the asymptotic normality of the transformed wavelet coherence, which ensures that, under the null hypothesis of $r_{ij}^{(a)} = r_{ij}^{(b)}$ (i.e., no change in synchronization), τ_{ij} has an asymptotic T distribution with $K - 1$ degrees of freedom. We employ the paired T test instead of the two-sample T test because $\hat{z}_{ijk}^{(a)}$ and $\hat{z}_{ijk}^{(b)}$ might be correlated as they are obtained from the same subject.

Fig. 3 shows the change detection results from two WP filters. As expected, significant increase in wavelet coherence is found in both low and high frequency bands over multiple scalp sites as cognitive binding occurs.

To further justify that the detected changes in synchronization pattern can be attributed to cognitive binding, we apply the same method to an attention control experiment,

in which each subject was presented with a slow sound-pulse train of variable duration, and the first EEG segment was taken immediately after the presentation and the second segment was taken just before the subject realized that the pulse train had stopped. Fig. 4 shows the change detection results from the same two WP filters as used in Fig. 3. The EEG synchronization patterns do not change significantly, as expected, because the thought of the subjects was effectively controlled (no cognitive binding) in this experiment.

7. Conclusions

In this research we have developed an STFA framework for synchronization analysis and change detection of multiple EEG signals. Wavelet coherence and wavelet partial coherence are proposed to quantify the pairwise synchronization and are applied to an ambiguous figure experiment to test for the hypothesis of cognitive binding. Significant increase in synchronization is found during the cognitive binding process in multiple frequency bands over multiple scalp sites. More sophisticated relationships among multiple scalp sites can be analyzed by using the multiple correlation coefficients and the canonical correlation analysis of the WP filtered EEG signals.

References

- [1] S. Bressler, R. Coppola, and R. Nakamura, “Episodic multi-regional cortical coherence at multiple frequencies during visual task performance,” *Nature*, vol. 338, pp. 334–337, 1993.
- [2] W. Singer, “Synchronization of cortical activity and its putative role in information processing and learning,” *Ann. Rev. Physiol.*, vol. 55, pp. 349–374, 1993.
- [3] B. Schack and W. Krause, “Instantaneous coherence as a sensible parameter for considering human information processing,” *Proc. IEEE Int. Conf. Pattern Recognition*, pp. 45–49, 1996.
- [4] D.L. Sherman, Y.C. Tsia, L.A. Rossell, M.A. Mirski, and N.V. Thakor, “Spectral analysis of a thalamus-to-cortex seizure pathway,” *IEEE Trans. Biomed. Eng.*, vol. 44, pp. 657–664, 1997.
- [5] I. Crock and S. Palmer, “The legacy of Gestalt psychology,” *Scientific American*, p. 84, December 1990.
- [6] T.H. Li, “Discrimination of time series by parametric filtering,” *J. Amer. Statist. Assoc.*, vol. 91, pp. 284–293, 1996.
- [7] M. Vetterli and J. Kovačević, *Wavelets and Subband Coding*, Upper Saddle River, NJ: Prentice-Hall, 1995.
- [8] D.R. Brillinger *Time Series: Data Analysis and Theory*, San Francisco: Holden-Day, 1981.
- [9] G. Saevarson, J.R. Sveinsson, and J.A. Benediktsson, “Wavelet-package transformation as a preprocessor of EEG waveforms for classification,” *Proc. IEEE Int. Conf. Eng. Med. Biology Soc.*, pp. 1305–1308, 1997.
- [10] A.B. Geva and D.H. Kerem, “Forecasting generalized epileptic seizures from the EEG signal by wavelet analysis and dynamic unsupervised fuzzy clustering,” *IEEE Trans. Biomed. Eng.*, vol. 45, pp. 1205–1216 1998.
- [11] K.R. Klemm, T.H. Li, and J.L. Hernandez, “Coherent EEG indicators of cognitive binding during ambiguous figure tasks,” *Consciousness and Cognition*, vol. 9, pp. 66–85, 2000.
- [12] T.W. Anderson, *An Introduction to Multivariate Statistical Analysis*, p. 24, New York: Wiley, 1984.

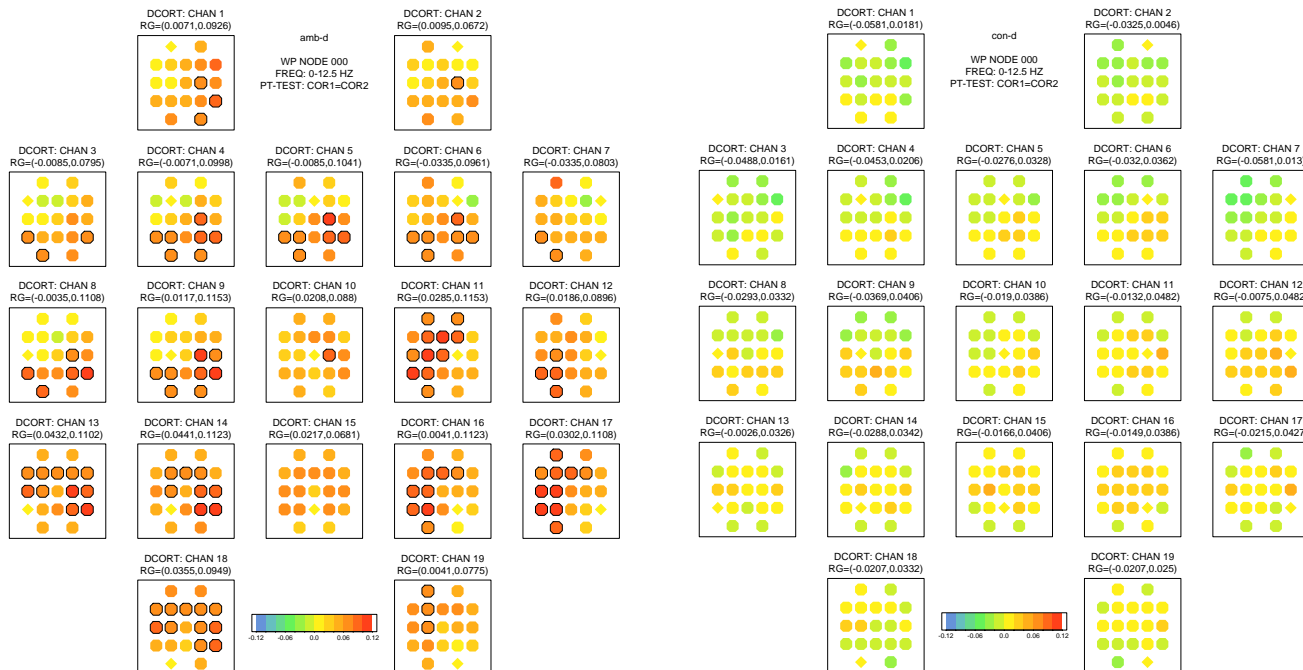


Figure 3. Wavelet coherence maps for synchronization change detection in the ambiguous figure experiment. Top: plot of $\bar{z}_{ij}^{(d)}(\mathcal{W}_{000})$. Bottom: plot of $\bar{z}_{ij}^{(d)}(\mathcal{W}_{011})$. Symbols outlined in black indicate significant coherence change at level 0.01.

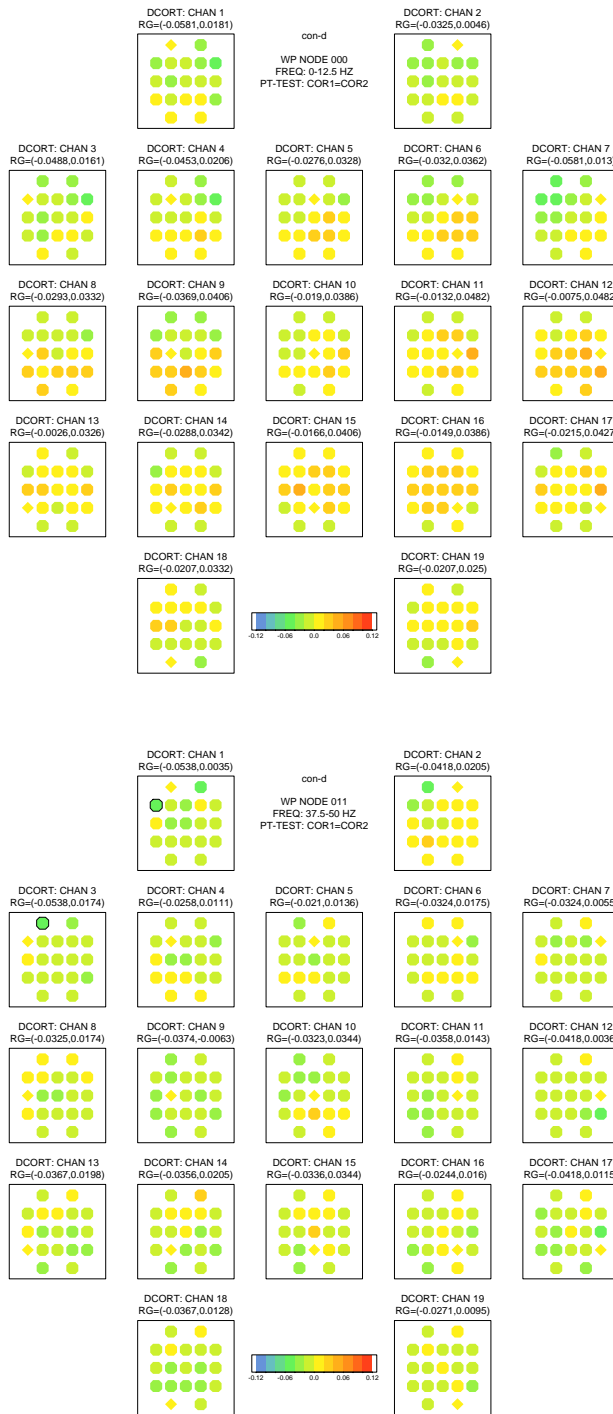


Figure 4. Same as Fig. 3, but for the attention control experiment.